



---

# A Sensitivity Study of the Design Parameters Affecting the Global Stability of Buckling-Restrained Braced Frames

*B. Saxey*

CoreBrace, Salt Lake City, USA

## **ABSTRACT**

Significant recent research has focused on the ability of buckling-restrained braces and their connections to act together as a series of resisting elements resisting mechanism formation. The potential failure mode associated with this mechanism formation is known as BRBF global stability and is required to be considered in the latest version of the AISC 341 Seismic Provisions (2022). A global stability analysis can be considerably more complex and require analysing more parameters of the BRB and connecting members than has commonly been performed by industry standards. It can be difficult for the design engineer to know how each of these parameters affects the global stability, which might be most efficient to change, and the proper bounds in which these parameters may be changed. This paper examines the components of the global stability model and the sensitivity of the system to varying each of these components in isolation. The varied parameters include, gusset thickness, gusset length, casing stiffness, insertion zone length and gap, neck compressive capacity, and others. It compares the results of the analytical method to a series of traditional design checks which consider the stability of elements of the BRBF independent from each other. These independent design checks are commonly used in industry for the design of BRB in the absence of (or in addition to) the global stability checks. Both sets of analyses are based on the design of a full-scale physical test performed by the author.

## **1 INTRODUCTION**

Buckling-restrained braced frames (BRBF) have been utilized world-wide as a cost-effective and reliable lateral-force resisting system for over two decades. The system is able to dissipate considerable seismic energy through axial yielding of the BRB's steel core in tension and in compression. For the element to perform properly, the members connecting the BRB core to the steel frame of the BRBF, including elements of the BRB itself, must be able to withstand the high forces they are required to transfer to the core without

buckling, fracturing, or otherwise performing in ways that would be detrimental to the system. Traditionally, these elements have been evaluated with independent checks of elements such as the BRB restrainer (casing), gusset plates, and BRB connecting elements – that is, checks of an element that don't directly consider other elements in the system. Checks and empirical limits established from BRB qualification testing are also commonly incorporated in these checks. Newly developed research by Matsui et al. (2010) and Takeuchi et al. (2014) consider the combined effects of these elements together acting as a system with plastic hinges forming that lead to instability. Dowswell (2016) proposed a simplification of this method utilizing a notional load yield line (NLYL) method. This method was further refined and formalized by Zaboli et al (2018). While this simplified method remains somewhat complex, it can be readily incorporated by practicing engineers and/or BRB manufacturers when sufficient information about the BRB is known. This method, its sensitivity to changes in input parameters and assumptions, and comparisons of its results to those of the more conventional independent design checks are reviewed in this paper.

## 2 EVALUATION METHOD

The NLYL methods proposed by Dowswell and formalized by Zaboli considers two categories of mechanism formation that can develop, leading to instability. See the buckled shapes in Figure 1. The first category is termed by Zaboli “over the yield-line” (OYL) and occurs when the brace buckles in the out-of-plane direction and forms a plastic hinge at the end of the restrainer and a second hinge at the gusset in a bendline occurring beyond the end of the BRB. The second category is termed “under the yield line” (UYL) and occurs when the BRB moves out of plane without a plastic hinge forming at the end of the restrainer. In this category, two plastic hinges form in the gusset plate, with one at the bendline beyond the end of the BRB and another hinge forming at the gusset connection to the structure. This UYL mode is similar to traditional gusset buckling but accounting for the destabilizing effects of the BRB acting upon it. Within these two categories, mechanisms can form in symmetrical, asymmetrical, or one-sided modes. From the equations for each of these modes however, it is evident that the lowest energy required is for the asymmetrical mode and therefore only that mode will be considered in this paper. Figure 1 shows the asymmetrical mode and assumed plastic hinge locations of the OYL and UYL collapse mechanisms. Terms used in their analysis are also provided in this figure. For the remainder of this paper, references to the OYL or UYL failure modes are referring specifically to the asymmetrical modes only.

### 2.1 NLYL evaluation method

The capacity of these mechanisms to resist plastic hinge formation, and the determination of the critical buckling load, is determined from Equations (1) and (2) as shown below.

$$N\xi L_0 \delta_s \leq (1 - 2\xi)M_p^g + M_p^r \quad (OYL - asymmetrical mode) \quad (1)$$

$$NL_{ave} \delta_s \leq (2 - 2\eta)M_p^g \rightarrow M_p^g \geq \frac{NL_{ave} \delta_s}{(2-2\eta)} = M_y^* \quad (UYL - asymmetrical mode) \quad (2)$$

Where  $N$  = the notional load at brace end on the yield line;  $\delta_s$  = moment amplification factor to account for second-order effects;  $M_p^g$  = reduced plastic moment capacity of gusset plate including axial force effect; and  $M_p^r$  = the moment restrainer capacity,  $\xi$  and  $\eta$  are destabilizing factors relating to the geometry of the brace and gusset within each mode. The reader is referred to Matsui, Takeuchi, Dowswell, Zaboli, and the text by Takeuchi & Wada (2017) for further definitions of these terms. The remainder of the terms in Equations 1 and 2 are defined in Figure 1.

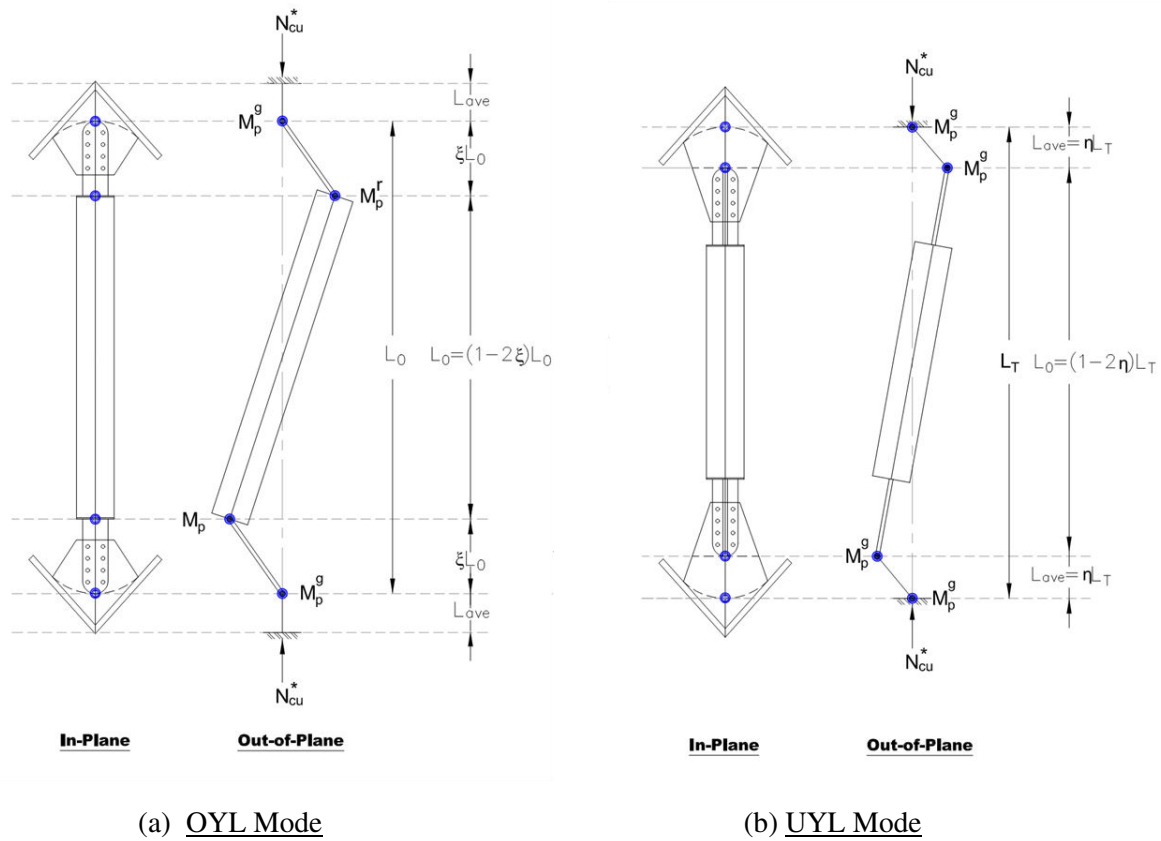


Figure 1: Asymmetrical Modes of Global Stability Mechanism Formation.

Both the left-hand side (within the terms  $N$  and  $\delta_s$ ) and the right-hand side (within the terms  $M_p^g$  and  $M_p^r$ ) are functions of the critical buckling load  $N_{cu}^*$ , and thus solving for the critical buckling load is not straightforward and must use numerical methods. However, if a known force is to be evaluated (such as the adjusted brace strength of the BRB), Equations 1 and 2 can be rearranged to provide a capacity ratio as follows:

$$\frac{N\xi L_0 \delta_s}{(1-2\xi)M_p^g + M_p^r} \leq 1.0 \quad (\text{OYL} - \text{asymmetrical mode}) \quad (3)$$

$$\frac{M_y^*}{M_p^g} \leq 1.0 \quad (\text{UYL} - \text{asymmetrical mode}) \quad (4)$$

In the format of Equations 3 and 4, the stability of the system can be evaluated as a capacity ratio for a given load,  $N^*$  (replacing  $N$ ), where values less than 1.0 represent stable designs. It is important to note that these “stability ratios” are not linear demand-capacity ratios in the sense that a stability ratio of 0.9, for example, does not mean that the demand can be increased by 10% before the ratio will exceed unity. As is common with stability analyses, a small change in load can produce a large change in the stability ratio (causing the analysis “blow up”). However, the global stability ratio can be used to determine if a particular configuration and set of loads remains stable and to compare with the results of traditional analysis methods. For brevity, the stability ratios will be referred to as ‘D/C’ ratios in the text, tables and figures of this paper. Plots showing the resulting D/C ratios for the NYLY stability ratios may be of different slope or different shape than plots of D/C ratios of more conventional design checks, but the points where each exceeds unity will be the focus and offer means to compare the methods.

## 2.2 Independent Evaluation Method

Independent evaluation of BRB consist of evaluating many, if not all of the elements evaluated in the NLYL method, and perhaps more. In addition to these items, design limits established from BRB qualification testing are also often adhered to. Items that will be considered in this paper are provided below. A detailed description of these checks if beyond the scope of this paper.

### 2.2.1 Restrainer buckling

The restrainer, or casing, of a BRB is an RHS, SHS, or CHS-type member which is checked for buckling using the well-known Euler buckling equations. Limits, or factors of safety, are often placed on this buckling capacity. One such limit is to use a factor to account for initial out of straightness of the casing member. For this study, this factor is taken as 0.877 which is common in practice. In addition to this, a  $\phi = 0.9$  is applied to casing buckling and the resulting effective factor of safety on casing buckling is  $1/(0.9*0.877) = 1.27$ . Note that the term ‘factor of safety’ is used here for illustrative purposes only, but the terms are employed as traditional phi-factors.

Additionally, casings are checked for out-of-plane and self-weight deflections (henceforth termed “OOP buckling”) resulting from their out-of-straightness and in addition to the seismic effect on their own self-weight. The method employed for this check is provided by Xie (2005) and considers various load combinations in analysing the critical limits on the casing member by applying axial, gravity, and out-of-plane forces on it. These limits are similar to what might be expected in a beam-column analysis with an axial load and bi-axial bending.

For the purposes of this paper, the greater of the Euler buckling capacity ratio and the OOP casing capacity ratio will be reported. Generally, the Euler buckling ratio controls for short brace lengths and the OOP capacity controls for moderate to long braces.

### 2.2.2 Gusset buckling

Gusset buckling provisions are well-known and are provided by Thornton (1984), Thornton & Lini (2011), and in Dowswell (2006) and (2012). These methods rely on calculating the Whitmore stress section and unbraced lengths over which buckling of the gusset plate under the applied loading is considered. In addition to these checks, out-of-plane buckling is checked on the gusset. These methods have been employed by BRB manufacturers for years and consist of calculating the total bendline length, the gusset section modulus over this length, an assumed out-of-plane story-drift angle of the frame and a notional load resulting from the perpendicular component of the axial load at this out-of-plane angle. The section capacity is then checked for bending using the section properties and the notional load. For purposes of this paper’s comparisons, the OOP story drift angle for this check is 2.5% to be consistent with New Zealand practice.

### 2.2.3 Connection limit checks

The final set of checks that will be considered are a group of checks that will be collectively known as “Connection Limit Checks.” These checks consist of many common checks, and other less well-known ones, that affect the final sizes of BRB connection elements. These checks include such common checks as, bolt bearing, shear and slip (slip considered at yield); gusset and connecting lug block rupture; tension rupture at connection lug; section gross yielding and net rupture capacity at neck; elastic and combined buckling at neck section, elastic buckling at connection region (without influence of gusset plate); and a cantilever buckling check ( $K=2.0$ ) on the section extending from the tip of brace to the start of the casing. This final check is often attributed to Nakamura and is provided in Bruneau, et al. (2011). It assumes the bending-moment transfer capacity at the casing ends are lost or neglected and further assumes a symmetric buckling mode. This cantilevered buckling check is a simplified attempt at checking the effects that global stability more aptly addresses and has been found by the author to be overly conservative in many cases.

### 3 EVALUATION OF NYLY METHOD AND COMPARISON TO INDEPENDENT DESIGN CHECKS

For purposes of comparing the NYLY method and evaluating its sensitivity to its various input parameters, a sample specimen was selected. The sample specimen chosen is depicted in Figure 2. This sample has an 1110 kN yield capacity and was chosen because it has been part of an extensive, multi-year study on BRB fatigue as reported by Saxey, et al. (2019), (2020) and because its loading pushes the limits of the NYLY method. Several identical specimens were tested in this fatigue study with the most severe compressive loading occurring in the test specimen with designation 1100-EQ1 (Saxey (2020)). This sample has an 1112 kN yield capacity and was tested in simulated earthquake responses for the 1989 Loma Prieta (1.2 x MCE) and 1985 Hector Mine (1.0 x MCE) to peak compressive loads of 2320 kN (2.09 x yield). Each run consisted of one Loma Prieta record, one Hector Mine record and one reversed Hector Mine record and the set of three EQ records was repeated until fracture – which occurred on the first Hector Mine record of the 4<sup>th</sup> run (i.e. the 11<sup>th</sup> total EQ record). This specimen had a 222 mm CHS casing with a thickness of 6.35 mm. However, a casing thickness of 9.53mm was used in the study, for the reasons given in section 3.3. The overall BRB length ( $L_0$ ) was 5800 mm, gussets were 32mm thick and gusset stiffeners were not employed.

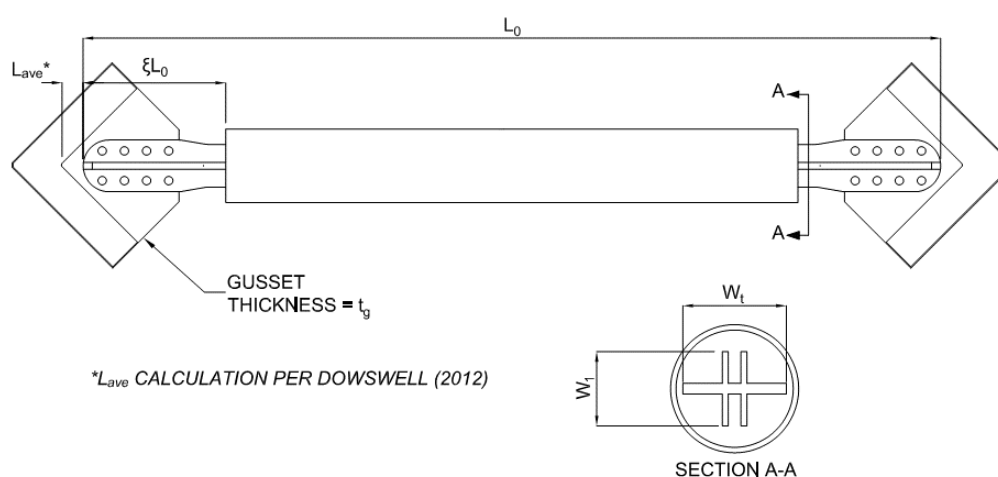


Figure 2: Sample specimen (Saxey, et al).

The comparisons below will vary one parameter of the NYLY method and compare the effects on the resulting capacity ratios to those resulting from the independent design checks (IDC) when the same variables are modified. The “base” design reported in each segment will be that from the original tested design (with the exception of the restrainer thickness as discussed below). Results will be plotted with values on the x-axis normalized to the base design unless noted otherwise. Parameters to be varied include, applied load ( $N^*$ ); overall BRB length ( $L_0$ ); restrainer elastic buckling capacity including gusset effect ( $N_{cr}^B$ ); gusset thickness ( $t_g$ ); brace effective length factor ( $k_b$ ) as can be affected by gusset stiffness; neck width in the OOP direction ( $W_t$ ); neck height ( $W_1$ ); extension length beyond casing each end ( $\xi L_0$ ); effective gusset buckling length ( $L_{ave}$ ); insertion zone embedment ratio; and the initial imperfection angle of the insertion zone ( $\theta_0$ ) made up primarily of the manufacturer’s debonding gap. Phi factors are used consistently between the methods.

#### 3.1 Varying Applied Load ( $N^*$ )

The first set of checks that was considered, and one of the most fundamental, is varying the applied load. Table 3 presents the results of varying the applied axial load  $\pm 20\%$ . The baseline case is shown in the first

row, and again at the 0% variant. The upper half provides measurements of the different parameters with the heading for the varied parameter ( $N^*$ ) is shaded. Capacity ratios are provided in the lower half, with those that exceed 1.0 shaded. Within the lower half of the table, capacity ratios for the NLYL method are on the left half and those for the independent evaluation methods are on the right half, with the controlling of these independent checks repeated in the right-most column. For the NLYL method, each analysis was done with  $K_b=1.0$  (unless this was the varied parameter) and again for  $K_b=0.7$  (this parameter is never varied) to highlight the effect of proving a sufficiently stiff gusset or otherwise reducing the brace effective length

*Table 1: Effects of varying applied load ( $N^*$ ).*

Parameters Considered											
Variant	$N^*$	$L_0$	$N_{cr}^B$	$t_g$	$K_b$	$W_t$	$W_1$	$\xi_{L_0}$	$L_{AVE}$	Embed Ratio	$\theta_0$
	kN	mm	kN	mm		mm	mm	mm	mm		rad
Base	2320	5741	3753	32	1.0	144	158	552	67	2.50	0.0071
-20%	1856	5741	3753	32	1.0	144	158	552	67	2.50	0.0071
-16%	1949	5741	3753	32	1.0	144	158	552	67	2.50	0.0071
-12%	2041	5741	3753	32	1.0	144	158	552	67	2.50	0.0071
-8%	2134	5741	3753	32	1.0	144	158	552	67	2.50	0.0071
-4%	2227	5741	3753	32	1.0	144	158	552	67	2.50	0.0071
0%	2320	5741	3753	32	1.0	144	158	552	67	2.50	0.0071
+4%	2413	5741	3753	32	1.0	144	158	552	67	2.50	0.0071
+8%	2505	5741	3753	32	1.0	144	158	552	67	2.50	0.0071
+12%	2598	5741	3753	32	1.0	144	158	552	67	2.50	0.0071
+16%	2691	5741	3753	32	1.0	144	158	552	67	2.50	0.0071
+20%	2784	5741	3753	32	1.0	144	158	552	67	2.50	0.0071

Variant	Capacity Ratios - NLYL Method				Capacity Ratios - Independent Design Checks (IDC)			
	D/C <sub>OYL</sub>	D/C <sub>OYL</sub> (Stiff Gst)	D/C <sub>UYL</sub>	D/C <sub>UYL</sub> (Stiff Gst)	D/C <sub>Rstr Bkl</sub>	D/C <sub>Guss Bkl</sub>	D/C <sub>Conn</sub>	Max D/C <sub>IDC</sub>
Base	0.97	0.36	0.09	0.07	1.00	0.70	0.99	1.00
-20%	0.44	0.23	0.05	0.04	0.80	0.57	0.80	0.80
-16%	0.51	0.25	0.06	0.05	0.84	0.59	0.84	0.84
-12%	0.60	0.27	0.06	0.05	0.88	0.62	0.87	0.88
-8%	0.70	0.30	0.07	0.06	0.92	0.65	0.91	0.92
-4%	0.82	0.33	0.08	0.07	0.96	0.68	0.95	0.96
0%	0.97	0.36	0.09	0.07	1.00	0.70	0.99	1.00
+4%	1.17	0.40	0.10	0.08	1.04	0.73	1.03	1.04
+8%	1.41	0.43	0.11	0.09	1.08	0.76	1.07	1.08
+12%	1.73	0.48	0.12	0.10	1.12	0.79	1.11	1.12
+16%	2.16	0.53	0.13	0.11	1.16	0.81	1.15	1.16
+20%	2.75	0.58	0.15	0.13	1.20	0.84	1.19	1.20
Max	<b>2.75</b>	<b>0.58</b>	<b>0.15</b>	<b>0.13</b>	<b>1.20</b>	<b>0.84</b>	<b>1.19</b>	<b>1.20</b>

factor. This is done for both the OYL and UYL modes. The controlling of the OYL and UYL at the appropriate  $K_b$  factor would control design, but they have been plotted independently to highlight how each is affected by the changes being investigated. This presentation of the data and the accompanying formatting will be used throughout this paper.

Figure 3 presents the results of Table 1 showing the maximum of the IDC and the capacity ratios for the OYL and UYL, each with the standard  $K_b$  and  $K_b = 0.7$  (the latter denoted as ‘Stiff Gst’). X-axis values in this figure are normalized to the base value. A dashed red line at the capacity limit ( $D/C = 1.0$ ) is also provided for reference. From this figure and Table 1 it is seen that IDC presents a very slightly more critical case at the base value but the results are both in very good agreement with respect to the point of unacceptable results. The NLYL method shows more sensitivity to increases in applied loads than does the IDC but again, this is a nature of the stability ratio of the method. The UYL checks and the OYL check with the stiffened gusset all indicate stability throughout the considered loading ranges. The IDC checks were controlled by OOP buckling of the restrainer per Xie, as indicated in Table 1. These limits were followed closely by connection limit states with the controlling limits being elastic and buckling checks at the neck section. Note that the peak value of the OYL check of 2.75, not shown on the figure for scale, required only an additional 20% increase in force to reach.

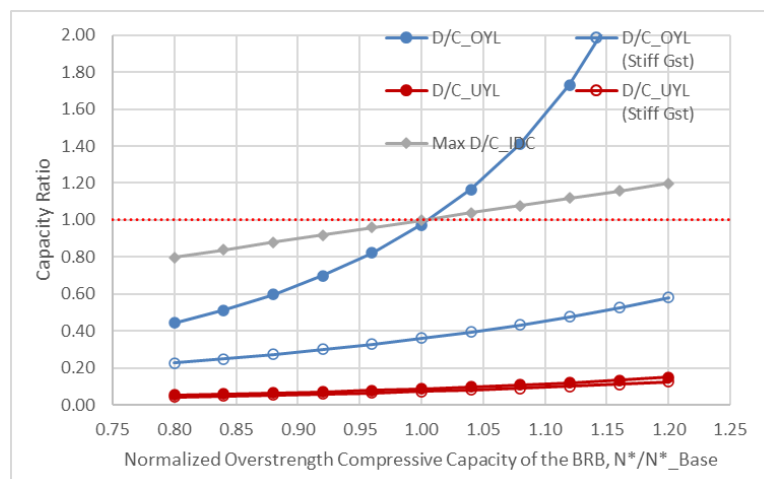


Figure 3: Effects of varying applied load ( $N^*$ ).

### 3.2 Varying Overall Brace Length ( $L_0$ )

Table 2 and Figure 4 present the results of varying the overall brace length,  $L_0$ ,  $\pm 20\%$  - also a fundamental design parameter. As can be seen, the OYL mode is sensitive to increases in length for the  $K_b = 1.0$  case. Again, good correlation with the IDC is seen with both predicting instability just beyond the baseline length. The OYL mode with stiffened gussets also shows sensitivity to change in length, but for the conditions considered, it remains below the stability limit indicating that gussets stiffened sufficiently to reduce the brace effective length ( $K_b = 0.7$ ) provide considerable design improvement over the unstiffened cases. The UYL results are significantly below the capacity limit indicating that gusset buckling, as expected, is not considerably sensitive to changes in brace length. At the largest increases in brace length, a beginning of separation between the two UYL cases can be seen implying that at very long lengths sensitivity of this case would begin to occur. The IDC method was controlled by OOP buckling of the restrainer beginning at the +4% variant. For consistency, an out of straightness factor of  $L/500$  is used in the Xie check and in the NLYL method. If  $L/1000$  were used, which is typical design per AISC, the IDC does not exceed the unity threshold until after the 1.13 variant (lengths greater than 1.13 x base length). The OYL check is also be

reduced but not significantly. Additional series for the OYL mode and the IDC checks are added to Figure 4 denoted as (L/1000) showing the effect. It is clear from these additional series that the OOP gusset buckling check is more sensitive to this out of straightness than is the NLYL method. This effect on the Xie restrainer check would also be present in the previous study varying  $N^*$ , but other limit states would control the IDC checks there with virtually not net change to Figure 3.

Table 2: Effects of varying overall brace length ( $L_0$ ).

Parameters Considered											
Variant	$N^*$	$L_0$	$N_{cr}^B$	$t_g$	$K_b$	$W_t$	$W_1$	$\xi_{L_0}$	$L_{AVE}$	Embed Ratio	$\theta_0$
	kN	mm	kN	mm		mm	mm	mm	mm		rad
Base	2320	5741	3753	32	1.0	144	158	552	67	2.50	0.0071
-21%	2320	4543	5992	32	1.0	144	158	552	67	2.50	0.0071
-17%	2320	4782	5407	32	1.0	144	158	552	67	2.50	0.0071
-13%	2320	5022	4904	32	1.0	144	158	552	67	2.50	0.0071
-8%	2320	5261	4467	32	1.0	144	158	552	67	2.50	0.0071
-4%	2320	5501	4087	32	1.0	144	158	552	67	2.50	0.0071
0%	2320	5741	3753	32	1.0	144	158	552	67	2.50	0.0071
+4%	2320	5980	3458	32	1.0	144	158	552	67	2.50	0.0071
+8%	2320	6220	3197	32	1.0	144	158	552	67	2.50	0.0071
+13%	2320	6459	2964	32	1.0	144	158	552	67	2.50	0.0071
+17%	2320	6699	2756	32	1.0	144	158	552	67	2.50	0.0071
+21%	2320	6938	2569	32	1.0	144	158	552	67	2.50	0.0071

Variant	Capacity Ratios - NLYL Method				Capacity Ratios - Independent Design Checks (IDC)			
	D/C <sub>OYL</sub>	D/C <sub>OYL</sub> (Stiff Gst)	D/C <sub>UYL</sub>	D/C <sub>UYL</sub> (Stiff Gst)	D/C <sub>Rstr Bkl</sub>	D/C <sub>Guss Bkl</sub>	D/C <sub>Conn</sub>	Max D/C <sub>IDC</sub>
Base	0.97	0.36	0.09	0.07	1.00	0.70	0.99	1.00
-21%	0.63	0.32	0.09	0.07	0.68	0.70	0.99	0.99
-17%	0.67	0.33	0.09	0.07	0.74	0.70	0.99	0.99
-13%	0.72	0.33	0.09	0.07	0.80	0.70	0.99	0.99
-8%	0.78	0.34	0.09	0.07	0.86	0.70	0.99	0.99
-4%	0.87	0.35	0.09	0.07	0.93	0.70	0.99	0.99
0%	0.97	0.36	0.09	0.07	1.00	0.70	0.99	1.00
+4%	1.12	0.37	0.09	0.07	1.07	0.71	0.99	1.07
+8%	1.34	0.39	0.09	0.07	1.15	0.71	0.99	1.15
+13%	1.68	0.40	0.09	0.07	1.23	0.71	0.99	1.23
+17%	2.30	0.42	0.09	0.07	1.31	0.71	0.99	1.31
+21%	3.73	0.44	0.09	0.07	1.40	0.71	1.00	1.40
Max	3.73	0.44	0.09	0.07	1.40	0.71	1.00	1.40

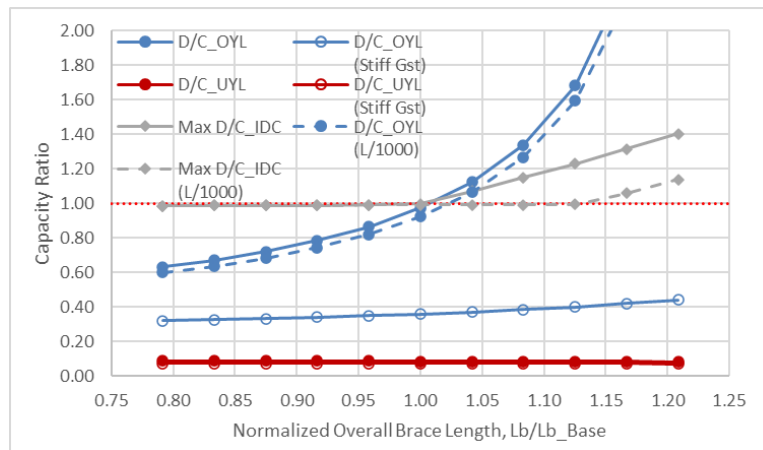


Figure 4: Effects of varying overall brace length ( $L_0$ ).

### 3.3 Varying BRB Elastic Buckling Capacity ( $N_{cr}^B$ )

Table 3 and Figure 5 present the results of varying the BRB restrainer moment of inertia by  $\pm 30\%$ . This range analysed is slightly larger than the previous 2 parameters because the lower bound closely represents one nominal size thinner restrainer wall thickness (6.35 mm) and the upper bound represents one size thicker restrainer wall thickness (12.7 mm) than the base design used in this study (9.53 mm). As noted previously, the physical brace, as reported in Saxey (2019) and (2020), used a 6.35 mm restrainer wall thickness which performed well in the testing, completing more than 10 earthquake records scaled to MCE or higher. However, the IDC and NLYL results both indicate that capacity is significantly exceeded at this level, suggesting conservatism in both methods. Additionally, NLYL analysis of the thinner restrainer wall thickness results in numerical instability if it is used as the base design and lower levels of  $N_{cr}^B$  are considered. As a result, the thicker restrainer wall thickness is used in this study but it should be noted that the -30% value shown in Table 3 and Figure 5, which reports a capacity ratio of 1.47 for the IDC method and 3.18 for the NLYL method (OYL mode), represents the actual restrainer stiffness used, which performed well in physical testing.

The results in Figure 5 show that both the NLYL and IDC methods predict unacceptable performance at the same level of restrainer stiffness, though the sensitivity of the NLYL method is higher. As noted previously, the Xie OOP restrainer check is sensitive to the level of out-of-straightness. If  $L/1000$  were used instead of  $L/500$ , the IDC check does not exceed unity until stiffnesses below the -0.82 variant and the DCR at the -0.7 variant, a stiffness consistent with the actual restrainer used in testing, is reduced to 1.16 (and 3.01 for the OYL mode). Again, two additional series have been added to Figure 5 showing the IDC and OYL results if  $L/1000$  were used. These results appear similar, as might be expected, to those for varying  $L_0$  observed in the previous section. If  $\phi$  is taken as 1.0, the IDC DCR is further reduced to 1.01 at the -0.7 variant showing a much better representation of the capacity seen in testing. Designs with stiffened gussets show significant performance improvements as seen in Figure 5, but as noted previously, gusset stiffeners were not used in the physical tests.

It is also noted that this restrainer was round as opposed to square restrainers that have been reported on in most studies of the NLYL and Takeuchi global stability methods. The reader is referenced to Matsui (2010) and the text by Takeuchi & Wada (2017) for calculating circular restrainer capacities, which are different than those for square restrainers.

Table 3: Effects of varying restrainer stiffness ( $N_{cr}^B$ ).

Parameters Considered											
Variant	$N^*$ kN	$L_0$ mm	$N_{cr}^B$ kN	$t_g$ mm	$K_b$	$W_t$ mm	$W_1$ mm	$\xi_{L_0}$ mm	$L_{AVE}$ mm	Embed Ratio	$\theta_0$ rad
Base	2320	5741	3753	32	1.0	144	158	552	67	2.50	0.0071
-30%	2320	5741	2627	32	1.0	144	158	552	67	2.50	0.0071
-24%	2320	5741	2852	32	1.0	144	158	552	67	2.50	0.0071
-18%	2320	5741	3077	32	1.0	144	158	552	67	2.50	0.0071
-12%	2320	5741	3303	32	1.0	144	158	552	67	2.50	0.0071
-6%	2320	5741	3528	32	1.0	144	158	552	67	2.50	0.0071
0%	2320	5741	3753	32	1.0	144	158	552	67	2.50	0.0071
+6%	2320	5741	3978	32	1.0	144	158	552	67	2.50	0.0071
+12%	2320	5741	4203	32	1.0	144	158	552	67	2.50	0.0071
+18%	2320	5741	4428	32	1.0	144	158	552	67	2.50	0.0071
+24%	2320	5741	4654	32	1.0	144	158	552	67	2.50	0.0071
+30%	2320	5741	4879	32	1.0	144	158	552	67	2.50	0.0071

Variant	Capacity Ratios - NLYL Method				Capacity Ratios - Independent Design Checks (IDC)			
	D/C <sub>OYL</sub>	D/C <sub>OYL</sub> (Stiff Gst)	D/C <sub>UYL</sub>	D/C <sub>UYL</sub> (Stiff Gst)	D/C <sub>Rstr Bkl</sub>	D/C <sub>Guss Bkl</sub>	D/C <sub>Conn</sub>	Max D/C <sub>IDC</sub>
Base	0.97	0.36	0.09	0.07	1.00	0.70	0.99	1.00
-30%	3.18	0.44	0.09	0.07	1.47	0.70	0.99	1.47
-24%	1.99	0.42	0.09	0.07	1.34	0.70	0.99	1.34
-18%	1.51	0.40	0.09	0.07	1.24	0.70	0.99	1.24
-12%	1.25	0.38	0.09	0.07	1.15	0.70	0.99	1.15
-6%	1.09	0.37	0.09	0.07	1.07	0.70	0.99	1.07
0%	0.97	0.36	0.09	0.07	1.00	0.70	0.99	1.00
+6%	0.89	0.35	0.09	0.07	0.94	0.70	0.99	0.99
+12%	0.83	0.34	0.09	0.07	0.88	0.70	0.99	0.99
+18%	0.78	0.34	0.09	0.07	0.84	0.70	0.99	0.99
+24%	0.74	0.33	0.09	0.07	0.79	0.70	0.99	0.99
+30%	0.71	0.33	0.09	0.07	0.76	0.70	0.99	0.99
Max	<b>3.18</b>	<b>0.44</b>	<b>0.09</b>	<b>0.07</b>	<b>1.47</b>	<b>0.70</b>	<b>0.99</b>	<b>1.47</b>

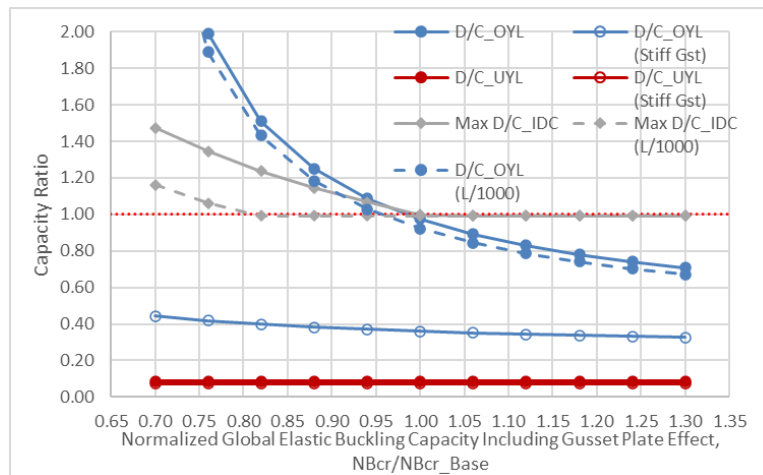


Figure 5: Effects of varying restrainer stiffness ( $N_{cr}^B$ ).

### 3.4 Varying Gusset Thickness ( $t_g$ )

Table 4 and Figure 6 show the results of varying the gusset thickness. A larger negative range was considered for this parameter in order to investigate variants that showed unacceptable results for the IDC checks and the UYL mode. Results show that the NLYL method (OYL mode) results in more conservative results than the IDC method (controlled by OOP gusset buckling). Both methods show similar sensitivity to changes in gusset thickness. The OYL mode is controlled by the reduced restrainer moment transfer capacity based on the capacity of the neck section considering axial effects,  $M_p^{r-neck}$ . While this capacity is not directly a function of the casing stiffness, the notional load of the OYL mode (the demand) is. As noted in the previous section this mode may tend to underpredict the contribution of the restrainer in providing stability. It is noted here that if the restrainer wall thickness were increased one nominal size, the OYL results exceed unity at essentially same point as the IDC results do. OYL results with this increased restrainer thickness are included in the plot in Figure 6 as the series denoted (Rest +1) indicating that the restrainer has been increased 1 nominal wall thickness beyond what is used for the other results in this section.

Also of interest, the NLYL method, as presented by Zaboli, uses the yield section of the neck for the calculation of  $M_p^{r-neck}$  if the gusset is unstiffened. This restriction is not seen in the global stability research by the Takeuchi group, but is used in this study. In Figure 6, yet an additional series is shown plotting the results for the OYL mode if the ultimate section capacity ( $F_u$ ) of the neck is used in calculating  $M_p^{r-neck}$  rather than the yield section capacity ( $F_y$ ). This series is denoted as (Neck Ult) and the results are nearly identical to those of the IDC checks in terms of where the unity threshold is exceeded. While using  $F_y$  for the capacity of  $M_p^{r-neck}$  results in good performance here, it is noted that better results are seen for other parameters discussed later, such as those for varying  $Wt$  and  $\xi L_0$ , using  $F_y$  for the section when unstiffened gussets are used. (The ultimate capacity is used for  $M_p^{r-neck}$  in all cases when the gussets are considered as sufficiently stiffened – in agreement with both the Zaboli and Takeuchi methods.)

The UYL mode does not show unacceptable results until thicknesses are considered that are below the -0.65 variant. As this method is primarily a check of gusset buckling, it is not surprising that this fairly compact gusset does not exceed capacity until a relatively thin gusset is considered.

Table 4: Effects of varying gusset thickness ( $t_g$ ).

Variant	Parameters Considered										
	N*	L <sub>0</sub>	N <sup>B</sup> <sub>cr</sub>	t <sub>g</sub>	K <sub>b</sub>	W <sub>t</sub>	W <sub>1</sub>	ξL <sub>0</sub>	L <sub>AVE</sub>	Embed Ratio	θ <sub>0</sub>
	kN	mm	kN	mm		mm	mm	mm	mm		rad
Base	2320	5741	3753	32	1.0	144	158	552	67	2.50	0.0071
-40%	2320	5741	3753	19	1.0	144	158	552	67	2.50	0.0071
-35%	2320	5741	3753	21	1.0	144	158	552	67	2.50	0.0071
-30%	2320	5741	3753	22	1.0	144	158	552	67	2.50	0.0071
-25%	2320	5741	3753	24	1.0	144	158	552	67	2.50	0.0071
-20%	2320	5741	3753	25	1.0	144	158	552	67	2.50	0.0071
-15%	2320	5741	3753	27	1.0	144	158	552	67	2.50	0.0071
-10%	2320	5741	3753	29	1.0	144	158	552	67	2.50	0.0071
-5%	2320	5741	3753	30	1.0	144	158	552	67	2.50	0.0071
0%	2320	5741	3753	32	1.0	144	158	552	67	2.50	0.0071
+5%	2320	5741	3753	33	1.0	144	158	552	67	2.50	0.0071
+10%	2320	5741	3753	35	1.0	144	158	552	67	2.50	0.0071

Variant	Capacity Ratios - NLYL Method				Capacity Ratios - Independent Design Checks (IDC)			
	D/C <sub>OYL</sub>	D/C <sub>OYL</sub> (Stiff Gst)	D/C <sub>UYL</sub>	D/C <sub>UYL</sub> (Stiff Gst)	D/C <sub>Rstr Bkl</sub>	D/C <sub>Guss Bkl</sub>	D/C <sub>Conn</sub>	Max D/C <sub>IDC</sub>
Base	0.97	0.36	0.09	0.07	1.00	0.70	0.99	1.00
-40%	2.29	0.70	1.57	1.32	1.00	1.42	1.01	1.42
-35%	2.02	0.64	0.75	0.63	1.00	1.26	1.01	1.26
-30%	1.79	0.59	0.45	0.38	1.00	1.14	1.00	1.14
-25%	1.60	0.54	0.30	0.25	1.00	1.03	1.00	1.03
-20%	1.43	0.49	0.22	0.18	1.00	0.95	1.00	1.00
-15%	1.29	0.45	0.17	0.14	1.00	0.87	1.00	1.00
-10%	1.17	0.42	0.13	0.11	1.00	0.81	1.00	1.00
-5%	1.07	0.39	0.11	0.09	1.00	0.75	0.99	1.00
0%	0.97	0.36	0.09	0.07	1.00	0.70	0.99	1.00
+5%	0.89	0.33	0.07	0.06	1.00	0.66	0.99	1.00
+10%	0.82	0.31	0.06	0.05	1.00	0.62	0.99	1.00
Max	2.29	0.70	1.57	1.32	1.00	1.42	1.01	1.42

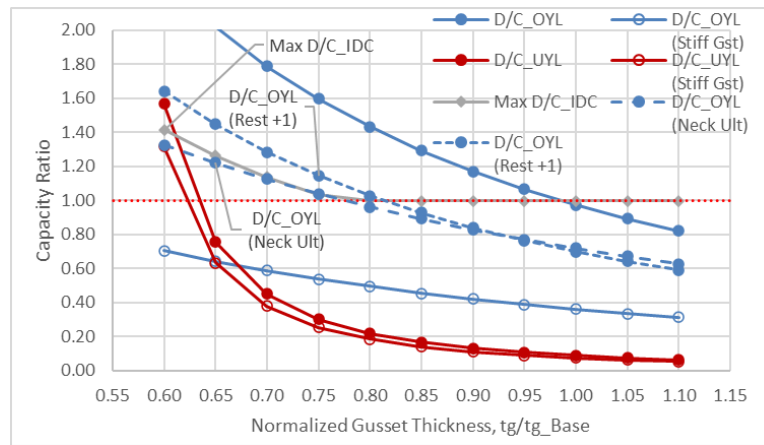


Figure 6: Effects of varying gusset thickness ( $t_g$ ).

### 3.5 Varying Brace Effective Length Factor ( $K_b$ )

The NLYL method uses an effective brace length factor which is applied directly to the BRB global elastic buckling capacity  $N_B^{cr}$  that was studied in a previous variant. That stiffness parameter includes the effect of the gusset plates and when the gusset plates are sufficiently stiff, a  $K_b$  factor of 0.7 is applied. If only one gusset is stiffened sufficiently, the  $K_b$  factor could be taken as 0.85. The resulting BRB stiffness directly affects the moment magnification factor,  $\delta_s$ , that is applied to the notional load to generate the OYL demand. Table 5 and Figure 7 provide the results of varying the BRB effective length factor,  $K_b$ . From these plots it is evident that the OYL mode is sensitive to changes in the  $K_b$  factor while the IDC method and the UYL mode are not. This presents a fundamental tenant of global stability calculations – that a stiffened gusset provides stability for the system as a whole. IDC methods do not have effective means of applying this concept. While the UYL mode is also not affected by the change in  $K_b$ , the OYL method varies from 0.63 to 3.38 over the range of -20% to +20%. This range is only 2/3 of the range applied for the consideration of both gussets stiffened, stressing the importance of ensuring that when a design assumes ‘stiffened gussets’ it must be ensured that the gussets are indeed sufficiently stiffened.

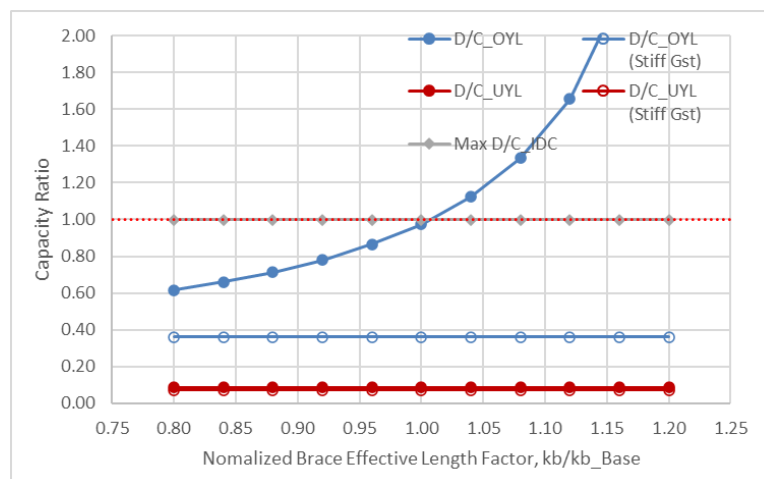


Figure 7: Effects of varying BRB effective length factor ( $K_b$ ).

Table 5: Effects of varying BRB effective length factor ( $K_b$ ).

Parameters Considered											
Variant	$N^*$ kN	$L_0$ mm	$N_{cr}^B$ kN	$t_g$ mm	$K_b$	$W_t$ mm	$W_1$ mm	$\xi_{L_0}$ mm	$L_{AVE}$ mm	Embed Ratio	$\theta_0$ rad
Base	2320	5741	3753	32	1.0	144	158	552	67	2.50	0.0071
-20%	2320	5741	5864	32	0.8	144	158	552	67	2.50	0.0071
-16%	2320	5741	5319	32	0.8	144	158	552	67	2.50	0.0071
-12%	2320	5741	4846	32	0.9	144	158	552	67	2.50	0.0071
-8%	2320	5741	4434	32	0.9	144	158	552	67	2.50	0.0071
-4%	2320	5741	4072	32	1.0	144	158	552	67	2.50	0.0071
0%	2320	5741	3753	32	1.0	144	158	552	67	2.50	0.0071
+4%	2320	5741	3470	32	1.0	144	158	552	67	2.50	0.0071
+8%	2320	5741	3217	32	1.1	144	158	552	67	2.50	0.0071
+12%	2320	5741	2992	32	1.1	144	158	552	67	2.50	0.0071
+16%	2320	5741	2789	32	1.2	144	158	552	67	2.50	0.0071
+20%	2320	5741	2606	32	1.2	144	158	552	67	2.50	0.0071

Variant	Capacity Ratios - NLYL Method				Capacity Ratios - Independent Design Checks (IDC)			
	D/C <sub>OYL</sub>	D/C <sub>OYL</sub> (Stiff Gst)	D/C <sub>UYL</sub>	D/C <sub>UYL</sub> (Stiff Gst)	D/C <sub>Rstr Bkl</sub>	D/C <sub>Guss Bkl</sub>	D/C <sub>Conn</sub>	Max D/C <sub>IDC</sub>
Base	0.97	0.36	0.09	0.07	1.00	0.70	0.99	1.00
-20%	0.62	0.36	0.09	0.07	1.00	0.70	0.99	1.00
-16%	0.66	0.36	0.09	0.07	1.00	0.70	0.99	1.00
-12%	0.71	0.36	0.09	0.07	1.00	0.70	0.99	1.00
-8%	0.78	0.36	0.09	0.07	1.00	0.70	0.99	1.00
-4%	0.86	0.36	0.09	0.07	1.00	0.70	0.99	1.00
0%	0.97	0.36	0.09	0.07	1.00	0.70	0.99	1.00
+4%	1.12	0.36	0.09	0.07	1.00	0.70	0.99	1.00
+8%	1.33	0.36	0.09	0.07	1.00	0.70	0.99	1.00
+12%	1.66	0.36	0.09	0.07	1.00	0.70	0.99	1.00
+16%	2.21	0.36	0.09	0.07	1.00	0.70	0.99	1.00
+20%	3.38	0.36	0.09	0.07	1.00	0.70	0.99	1.00
Max	<b>3.38</b>	<b>0.36</b>	<b>0.09</b>	<b>0.07</b>	<b>1.00</b>	<b>0.70</b>	<b>0.99</b>	<b>1.00</b>

### 3.6 Varying Out of Plane Neck Width ( $W_t$ )

Table 6 and Figure 8 provide the results of varying the width of the neck that is strong-axis in the OOP direction,  $W_t$ . Core extension stability considerations, in particular OOP buckling at the neck section, control the IDC method's capacity ratios. The OYL mode, without stiffened gussets, shows nearly the identical point of instability as the IDC method. Within the calculations of the OYL mode, the neck capacity,  $M_p^{r-neck}$  controls the design. Two important factors are noted here. First, good agreement is seen using the yield

capacity of the section when the gussets aren't stiffened, as recommended by Zaboli. This is in contrast to what was seen for varying the overall brace buckling capacity,  $N_{cr}^B$ . A series showing the results if the ultimate strength is used for calculating  $M_p^{r-neck}$  has been added to Figure 8. Second, the calculation of  $M_p^{r-neck}$  as given in Zaboli uses a method presented in Takeuchi based on an AIJ equation with a power of 2 term in it. While not stated expressly, both the equation and the power of 2 are specific to the cruciform section used in the Takeuchi research. For other sections, such as an H-shape or split cruciform sections that are common in BRB design, the appropriateness of both the equation and the power term must be verified. Using a PISA 3D analysis to create a P-M interaction curve, the authors have confirmed that both the equation and the power term used in Zaboli are not adequate for the neck section shown in Figure 2 and have created a more appropriate equation that is used in this study. The derivation of this equation is beyond the scope of this paper, but it is noted that the AIJ equation used in Zaboli will produce unconservative results. A plot of the results if the AIJ equation is used for the calculation of  $M_p^{r-neck}$  is also shown in Figure 8 and denoted (AIJ Eqn). Obviously, using both the ultimate strength and the AIJ equation would produce compounding levels of unconservatism to the results.

While the stiffened gusset version of the OYL mode shows sensitivity to varying the Wt section, it remains well within the capacity limit throughout the range of variants studied. At the extreme -20% variant considered, the neck section is at 88% of capacity for axial yielding only and it is unlikely that a smaller section could be worth considering. Again, it is seen that a stiff gusset provides stability for a section with a weaker neck. The UYL modes are not affected by the change in Wt as would be expected.

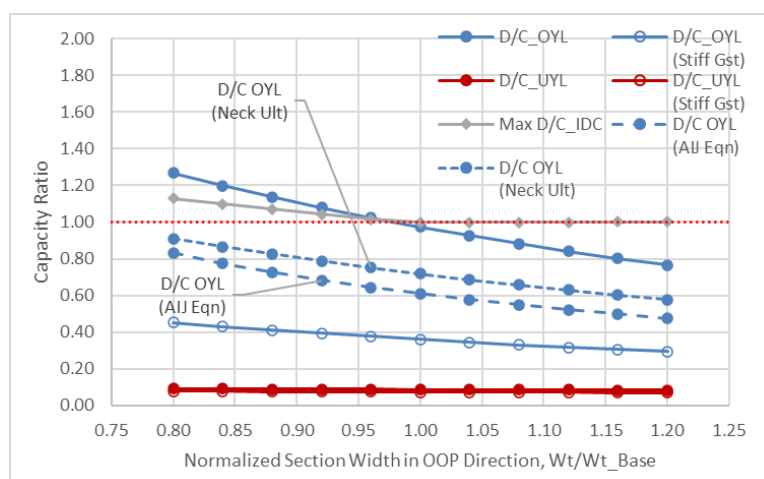


Figure 8: Effects of varying out-of-plane neck section width ( $W_t$ ).

Table 6: Effects of varying out-of-plane neck section width ( $W_t$ ).

Parameters Considered											
Variant	$N^*$	$L_0$	$N_{cr}^B$	$t_g$	$K_b$	$W_t$	$W_1$	$\xi L_0$	$L_{AVE}$	Embed Ratio	$\theta_0$
	kN	mm	kN	mm		mm	mm	mm	mm		rad
Base	2320	5741	3753	32	1.0	144	158	552	67	2.50	0.0071
-20%	2320	5741	3753	32	1.0	115	158	552	67	2.50	0.0088
-16%	2320	5741	3753	32	1.0	121	158	552	67	2.50	0.0084
-12%	2320	5741	3753	32	1.0	127	158	552	67	2.50	0.0080
-8%	2320	5741	3753	32	1.0	132	158	552	67	2.50	0.0077
-4%	2320	5741	3753	32	1.0	138	158	552	67	2.50	0.0074
0%	2320	5741	3753	32	1.0	144	158	552	67	2.50	0.0071
+4%	2320	5741	3753	32	1.0	150	158	552	67	2.50	0.0068
+8%	2320	5741	3753	32	1.0	155	158	552	67	2.50	0.0065
+12%	2320	5741	3753	32	1.0	161	158	552	67	2.50	0.0063
+16%	2320	5741	3753	32	1.0	167	158	552	67	2.50	0.0061
+20%	2320	5741	3753	32	1.0	173	158	552	67	2.50	0.0059

Variant	Capacity Ratios - NLYL Method				Capacity Ratios - Independent Design Checks (IDC)			
	D/C <sub>OYL</sub>	D/C <sub>OYL</sub> (Stiff Gst)	D/C <sub>UYL</sub>	D/C <sub>UYL</sub> (Stiff Gst)	D/C <sub>Rstr Bkl</sub>	D/C <sub>Guss Bkl</sub>	D/C <sub>Conn</sub>	Max D/C <sub>IDC</sub>
Base	0.97	0.36	0.09	0.07	1.00	0.70	0.99	1.00
-20%	1.27	0.45	0.09	0.08	1.00	0.70	1.13	1.13
-16%	1.20	0.43	0.09	0.08	1.00	0.70	1.10	1.10
-12%	1.14	0.41	0.09	0.08	1.00	0.70	1.07	1.07
-8%	1.08	0.39	0.09	0.07	1.00	0.70	1.04	1.04
-4%	1.02	0.38	0.09	0.07	1.00	0.70	1.02	1.02
0%	0.97	0.36	0.09	0.07	1.00	0.70	0.99	1.00
+4%	0.93	0.35	0.09	0.07	1.00	0.70	0.97	1.00
+8%	0.88	0.33	0.09	0.07	1.00	0.70	0.95	1.00
+12%	0.84	0.32	0.09	0.07	1.00	0.70	0.92	1.00
+16%	0.80	0.31	0.08	0.07	1.00	0.70	0.90	1.00
+20%	0.77	0.29	0.08	0.07	1.00	0.70	0.89	1.00
Max	<b>1.27</b>	<b>0.45</b>	<b>0.09</b>	<b>0.08</b>	<b>1.00</b>	<b>0.70</b>	<b>1.13</b>	<b>1.13</b>

### 3.7 Varying In-Plane Neck Width ( $W_1$ )

Table 7 and Figure 9 provide the results of varying the in-plane section width,  $W_1$ . The behaviour is in very good agreement with the IDC in that levels of unacceptable D/C are predicted at essentially identical points - i.e. at a load about 3% lower than the baseline. One noteworthy exception is the extreme jump seen for both OYL cases at the +20% variant. This is a result of the equations used to calculate the moment transfer capacity of the restrainer where the distance from the section to the restrainer wall is considered. For round restrainers this distance is more limited than it is for a square section. At the +20% variant, the  $W_1$  section is

nearing the restrainer wall to the point that calculated capacity quickly diminishes. This may be thought of as a localized failure of the restrainer wall. It is also noted that for this parameter and several others, the baseline design value is very close to that where the D/C ratio will be exceeded. This is not coincidental, but rather indicates that the BRB considered was designed very efficiently for the expected forces seen in testing.

Table 7: Effects of varying in-plane neck section width ( $W_1$ ).

Parameters Considered											
Variant	N*	$L_0$	$N_{cr}^B$	$t_g$	$K_b$	$W_t$	$W_1$	$\xi_{L_0}$	$L_{AVE}$	Embed Ratio	$\theta_0$
	kN	mm	kN	mm		mm	mm	mm	mm		rad
Base	2320	5741	3753	32	1.0	144	158	552	67	2.50	0.0071
-20%	2320	5741	3753	32	1.0	144	127	552	67	2.50	0.0071
-16%	2320	5741	3753	32	1.0	144	133	552	67	2.50	0.0071
-12%	2320	5741	3753	32	1.0	144	139	552	67	2.50	0.0071
-8%	2320	5741	3753	32	1.0	144	146	552	67	2.50	0.0071
-4%	2320	5741	3753	32	1.0	144	152	552	67	2.50	0.0071
0%	2320	5741	3753	32	1.0	144	158	552	67	2.50	0.0071
+4%	2320	5741	3753	32	1.0	144	165	552	67	2.50	0.0071
+8%	2320	5741	3753	32	1.0	144	171	552	67	2.50	0.0071
+12%	2320	5741	3753	32	1.0	144	178	552	67	2.50	0.0071
+16%	2320	5741	3753	32	1.0	144	184	552	67	2.50	0.0071
+20%	2320	5741	3753	32	1.0	144	190	552	67	2.50	0.0071

Variant	Capacity Ratios - NLYL Method				Capacity Ratios - Independent Design Checks (IDC)			
	D/C <sub>OYL</sub>	D/C <sub>OYL</sub> (Stiff Gst)	D/C <sub>UYL</sub>	D/C <sub>UYL</sub> (Stiff Gst)	D/C <sub>Rstr Bkl</sub>	D/C <sub>Guss Bkl</sub>	D/C <sub>Conn</sub>	Max D/C <sub>IDC</sub>
Base	0.97	0.36	0.09	0.07	1.00	0.70	0.99	1.00
-20%	1.32	0.42	0.09	0.07	1.00	0.70	1.14	1.14
-16%	1.23	0.41	0.09	0.07	1.00	0.70	1.11	1.11
-12%	1.15	0.39	0.09	0.07	1.00	0.70	1.08	1.08
-8%	1.08	0.38	0.09	0.07	1.00	0.70	1.05	1.05
-4%	1.03	0.37	0.09	0.07	1.00	0.70	1.02	1.02
0%	0.97	0.36	0.09	0.07	1.00	0.70	0.99	1.00
+4%	0.93	0.35	0.09	0.07	1.00	0.70	0.97	1.00
+8%	0.89	0.34	0.09	0.07	1.00	0.70	0.94	1.00
+12%	0.85	0.33	0.09	0.07	1.00	0.70	0.92	1.00
+16%	0.82	0.32	0.09	0.07	1.00	0.70	0.90	1.00
+20%	1.49	0.69	0.09	0.07	1.00	0.70	0.89	1.00
Max	1.49	0.69	0.09	0.07	1.00	0.70	1.14	1.14

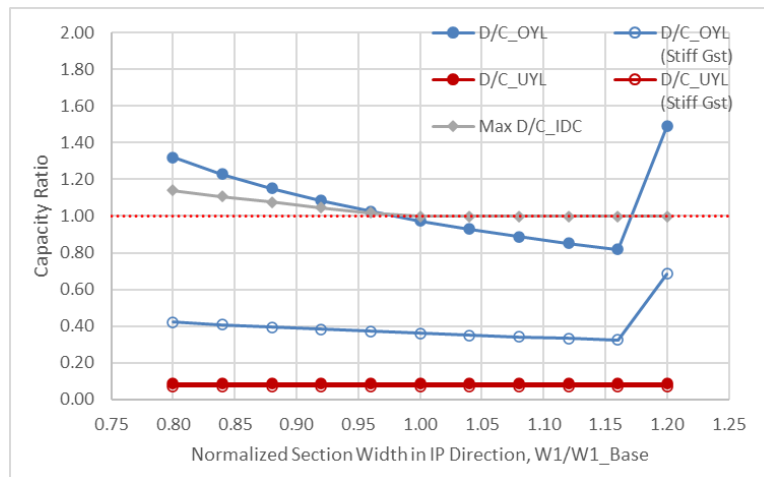


Figure 9: Effects of varying in-plane neck section width ( $W_1$ ).

### 3.8 Varying the Total BRB Extension Length Beyond Restrainer End ( $\xi L_0$ )

Results of varying the BRB extension length beyond the restrainer are shown in Table 8 and Figure 10. Variations somewhat greater than used for other parameters considered in this study due to the low sensitivity to changes. For this variation, the entire length from restrainer end to tip of brace (at both ends) was scaled up by changing each individual component (bolt spacing, edge distance, stroke, etc) to get the total change in length. As such, the gusset also grew with this change, but this change is limited to that portion of the gusset that is covered by brace connecting elements (i.e. not to the extension of the gusset beyond the tip of the BRB). This is considered representative of the NLYL method, which considers the  $\xi L_0$  over this entire region. Here again, core extension stability checks control the IDC checks and moment capacity of the neck ( $M_p^{r-neck}$ ) controls the OYL mode checks. Figure 10 shows that the two analysis methods show nearly identical points where unity is exceeded in the D/C ratios. Again, for comparison, results are provided in an additional series showing the case if  $M_p^{r-neck}$  were calculated using the AIJ equation. These variations in  $\xi L_0$  are likely greater than would be expected in typical design. The slight decrease in the UYL mode is due to the gusset capacity increasing as it gets larger (i.e. increased Whitmore section) which also reduces the moment magnification factor,  $\delta_s$ .

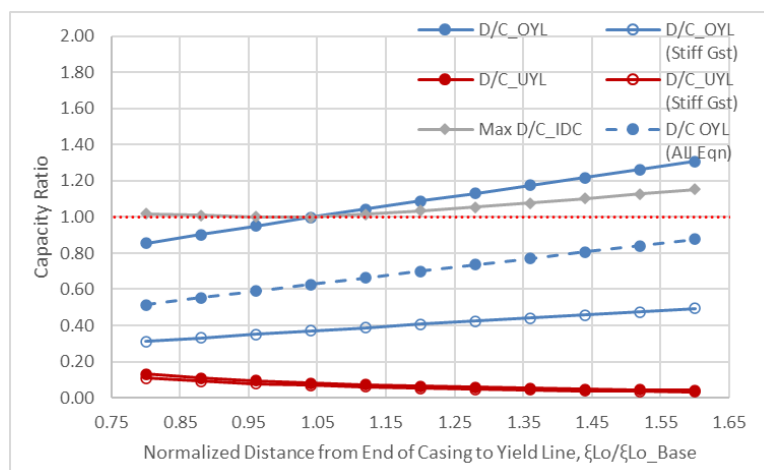


Figure 10: Effects of varying extension length beyond restrainer end ( $\xi L_0$ ).

Table 8: Effects of varying extension length beyond restrainer end ( $\xi L_0$ ).

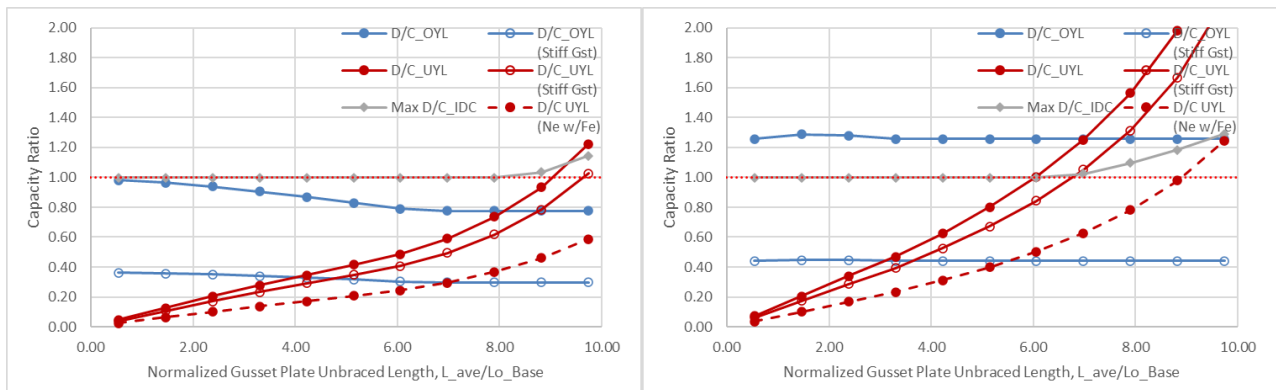
Parameters Considered											
Variant	N*	L <sub>0</sub>	N <sup>B</sup> <sub>cr</sub>	t <sub>g</sub>	K <sub>b</sub>	W <sub>t</sub>	W <sub>1</sub>	ξL <sub>0</sub>	L <sub>AVE</sub>	Embed Ratio	θ <sub>0</sub>
	kN	mm	kN	mm		mm	mm	mm	mm		rad
Base	2320	5741	3753	32	1.0	144	158	552	67	2.50	0.0071
-20%	2320	5721	3779	32	1.0	144	158	442	70	2.50	0.0071
-12%	2320	5729	3768	32	1.0	144	158	486	69	2.50	0.0071
-4%	2320	5737	3758	32	1.0	144	158	530	67	2.50	0.0071
+4%	2320	5744	3749	32	1.0	144	158	575	66	2.50	0.0071
+12%	2320	5750	3740	32	1.0	144	158	619	65	2.50	0.0071
+20%	2320	5756	3733	32	1.0	144	158	663	64	2.50	0.0071
+28%	2320	5761	3726	32	1.0	144	158	707	63	2.50	0.0071
+36%	2320	5766	3720	32	1.0	144	158	751	62	2.50	0.0071
+44%	2320	5770	3714	32	1.0	144	158	796	62	2.50	0.0071
+52%	2320	5774	3709	32	1.0	144	158	840	61	2.50	0.0071
+60%	2320	5778	3705	32	1.0	144	158	884	60	2.50	0.0071

Variant	Capacity Ratios - NLYL Method				Capacity Ratios - Independent Design Checks (IDC)			
	D/C <sub>OYL</sub>	D/C <sub>OYL</sub> (Stiff Gst)	D/C <sub>UYL</sub>	D/C <sub>UYL</sub> (Stiff Gst)	D/C <sub>Rstr Bkl</sub>	D/C <sub>Guss Bkl</sub>	D/C <sub>Conn</sub>	Max D/C <sub>IDC</sub>
Base	0.97	0.36	0.09	0.07	1.00	0.70	0.99	1.00
-20%	0.85	0.31	0.13	0.11	1.02	0.76	0.96	1.02
-12%	0.90	0.33	0.11	0.09	1.01	0.73	0.97	1.01
-4%	0.95	0.35	0.09	0.08	1.00	0.71	0.98	1.00
+4%	1.00	0.37	0.08	0.07	0.99	0.70	1.00	1.00
+12%	1.04	0.39	0.07	0.06	0.99	0.68	1.02	1.02
+20%	1.09	0.41	0.06	0.05	0.98	0.66	1.04	1.04
+28%	1.13	0.42	0.06	0.05	0.97	0.65	1.06	1.06
+36%	1.18	0.44	0.05	0.04	0.96	0.63	1.08	1.08
+44%	1.22	0.46	0.05	0.04	0.96	0.62	1.10	1.10
+52%	1.26	0.48	0.04	0.04	0.95	0.61	1.13	1.13
+60%	1.31	0.49	0.04	0.03	0.94	0.60	1.15	1.15
Max	<b>1.31</b>	<b>0.49</b>	<b>0.13</b>	<b>0.11</b>	<b>1.02</b>	<b>0.76</b>	<b>1.15</b>	<b>1.15</b>

### 3.9 Varying the Effective Gusset Buckling Length (L<sub>ave</sub>)

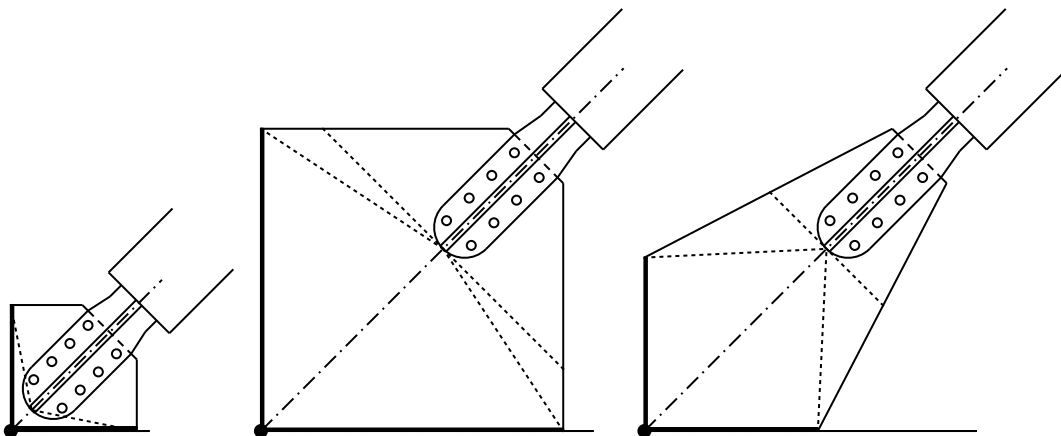
Table 9 and Figure 11a give the results of varying the extension length beyond the tip of the BRB, L<sub>ave</sub>, for gussets that are increased without taper (square gusset). Variations much greater those used for other variants were considered in order to produce results that exceeded acceptable limits. For the square gusset, it can be seen that the NLYL (UYL mode) and IDC methods produce similar results once the core extension limit states control the design of the IDC method but with the IDC method predicting unacceptable results a

variant sooner than the UYL mode. It is noted that the stiffened gusset version ( $K_b=0.7$ ) of the UYL mode also shows considerable sensitivity over the considered range with the stiffened gusset allowing the gusset to be extended roughly one variant further before unacceptable results are obtained. Figure 11b shows the results if the gusset is tapered to a  $30^\circ$  limit but otherwise the extension is the same. This produces a dramatic increase in the capacity ratio compared with the square gusset, as would be expected. In this case, the standard UYL mode produces unacceptable results at virtually the same point that the IDC does and the UYL with stiffened gussets produces unacceptable results less than a variant away. From Table 9, which includes the results for the square gusset only, the max extension is around 650 mm from the base value, which is considerable, but values for the tapered gussets exceed unity at around half this value. Designers may need to consider stiffened gussets when utilizing extended gussets especially if the gussets are tapered. Figure 12 shows the approximate shapes and bendline locations of the base design and the extreme case square and tapered gussets. It is noted that for the tapered gusset, the unstiffened gusset in the OYL mode exceeds unity at even the base value (test gussets were not tapered).. This capacity stays fairly constant throughout the range but with a slight increase and subsequent decrease between the first and fourth variants. This odd variation is a function of the bendline shape as it goes from tapered in towards the gusset to tapered out away from the gusset (as can be seen comparing Figure 12a and 12b) and then the controlling bendline changing over to the perpendicular bendline rather than the bendline extending to the gusset corner (these two bendline versions are clearly visible in Figure 12c).



(a)

(b)



(a)

(b)

(c)

Figure 12: Gusset shapes with varied  $L_{ave}$ : (a) base, (b) extreme extended square, (c) extreme tapered.

Table 9: Effects of varying effective gusset buckling length ( $L_{ave}$ ) – square gusset only.

Parameters Considered											
Variant	$N^*$ kN	$L_0$ mm	$N_{cr}^B$ kN	$t_g$ mm	$K_b$	$W_t$ mm	$W_1$ mm	$\xi L_0$ mm	$L_{AVE}$ mm	Embed Ratio	$\theta_0$ rad
Base	2320	5741	3753	32	1.0	144	158	552	67	2.50	0.0071
-46%	2320	5741	3753	32	1.0	144	158	552	36	2.50	0.0071
+46%	2320	5741	3753	32	1.0	144	158	552	97	2.50	0.0071
+138%	2320	5741	3753	32	1.0	144	158	552	159	2.50	0.0071
+230%	2320	5741	3753	32	1.0	144	158	552	220	2.50	0.0071
+322%	2320	5741	3753	32	1.0	144	158	552	281	2.50	0.0071
+414%	2320	5741	3753	32	1.0	144	158	552	343	2.50	0.0071
+506%	2320	5741	3753	32	1.0	144	158	552	404	2.50	0.0071
+598%	2320	5741	3753	32	1.0	144	158	552	465	2.50	0.0071
+690%	2320	5741	3753	32	1.0	144	158	552	527	2.50	0.0071
+782%	2320	5741	3753	32	1.0	144	158	552	588	2.50	0.0071
+874%	2320	5741	3753	32	1.0	144	158	552	649	2.50	0.0071

Variant	Capacity Ratios - NLYL Method				Capacity Ratios - Independent Design Checks (IDC)			
	D/C <sub>OYL</sub>	D/C <sub>OYL</sub> (Stiff Gst)	D/C <sub>UYL</sub>	D/C <sub>UYL</sub> (Stiff Gst)	D/C <sub>Rstr Bkl</sub>	D/C <sub>Guss Bkl</sub>	D/C <sub>Conn</sub>	Max D/C <sub>IDC</sub>
Base	0.97	0.36	0.09	0.07	1.00	0.70	0.99	1.00
-46%	0.98	0.36	0.05	0.04	1.00	0.70	0.99	1.00
+46%	0.96	0.36	0.13	0.11	1.00	0.71	0.99	1.00
+138%	0.94	0.35	0.20	0.17	1.00	0.72	0.99	1.00
+230%	0.91	0.34	0.28	0.23	1.00	0.73	0.99	1.00
+322%	0.87	0.33	0.35	0.29	1.00	0.75	0.99	1.00
+414%	0.83	0.32	0.41	0.35	1.00	0.78	0.99	1.00
+506%	0.79	0.30	0.48	0.41	1.00	0.82	0.99	1.00
+598%	0.77	0.30	0.59	0.50	1.00	0.88	0.99	1.00
+690%	0.77	0.30	0.74	0.62	1.00	0.95	0.99	1.00
+782%	0.77	0.30	0.93	0.78	1.00	1.04	0.99	1.04
+874%	0.77	0.30	1.22	1.03	1.00	1.14	0.99	1.14
Max	<b>0.98</b>	<b>0.36</b>	<b>1.22</b>	<b>1.03</b>	<b>1.00</b>	<b>1.14</b>	<b>0.99</b>	<b>1.14</b>

### 3.10 Varying the Embedment Ratio

Variations in the embedment ratio are shown in Table 10 and Figure 13. Note that the x-axis of Figure 13 is in terms of actual embedment ratio rather than the normalized ratio since comparing the actual value was considered to be more meaningful as particular thresholds of this value are often used directly in design (or

to justify design). Embedment ratios from the base value down to 1.0 were considered. The OYL mode begins to show unacceptable results at around an embedment ratio of 2.2 for the unstiffened gusset, higher than the value of 2.0 that is often considered as a maximum necessary for design. However, for this highly loaded BRB (with overstrength over 2.0x yield) a minimum value of 2.35 is needed for stability. While the embedment ratio affects the restrainer moment transfer capacity, which for this design is fully developed at an embedment ratio of 1.75, it also affects the imperfection angle which directly affects the notional load (Notional Load =  $N \cdot \theta_i$ ), which in this design required an embedment greater than 2.2 to keep this load sufficiently small. The IDC method does not use the embedment ratio expressly in design checks other than to limit this to recommended values as an empirical limit. Limits of 1.7 to 2.0 are typically used as this empirical limit and values less than 2.0 are shown shaded blue in the upper half of Table 10. However, as has just been shown, this may not always be sufficient. Of note, a dispersion angle (similar to Whitmore angle) of  $40^\circ$  is recommended in the NLYL method presented by Zaboli, but for consistency here with the IDC, which use values in accordance with AISC, a value of  $30^\circ$  is used throughout this study. Figure 13 has an added series with the results for the unstiffened gusset version of the OYL mode with the dispersion angle taken as  $40^\circ$ , denoted ( $\theta=40^\circ$ ). From these results it can be seen that acceptable results are found at embedment ratios as low as 1.9-2.0 which is more in-line with expected results. It is important to note that the analysis performed in this section ignores the increased overstrength that would result from the reduced yielding core length that would typically result from increasing the embedment length. In reality, the overstrength would increase the demands on the system, which would act in opposition to the benefits of increasing the embedment length. Thus, as with many aspects of BRB design, a balance must be achieved between these opposing actions.

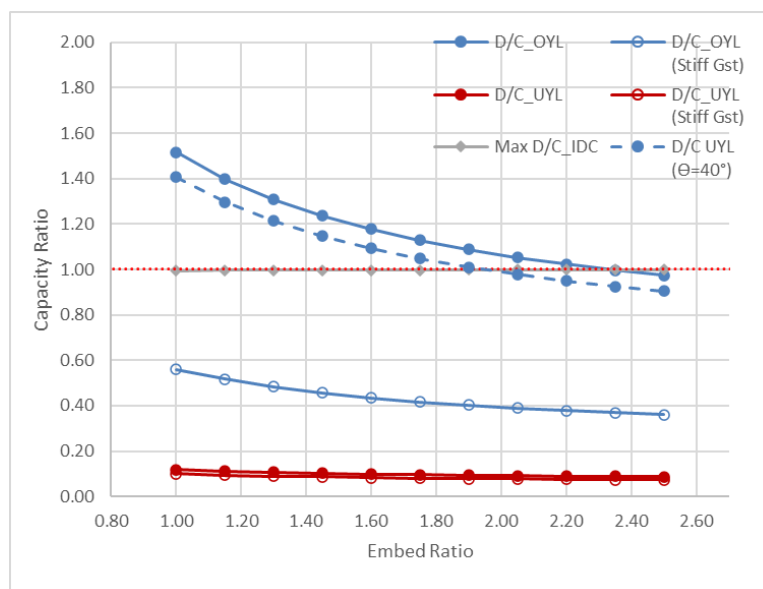


Figure 13: Effects of varying the embedment ratio.

Table 10: Effects of varying embedment ratio.

Parameters Considered											
Variant	N*	L <sub>0</sub>	N <sup>B</sup> <sub>cr</sub>	t <sub>g</sub>	K <sub>b</sub>	W <sub>t</sub>	W <sub>1</sub>	ξL <sub>0</sub>	L <sub>AVE</sub>	Embed Ratio	θ <sub>0</sub>
	kN	mm	kN	mm		mm	mm	mm	mm		rad
Base	2320	5741	3753	32	1.0	144	158	552	67	2.50	0.0071
-60%	2320	5741	3753	32	1.0	144	158	552	67	1.00	0.0177
-54%	2320	5741	3753	32	1.0	144	158	552	67	1.15	0.0154
-48%	2320	5741	3753	32	1.0	144	158	552	67	1.30	0.0136
-42%	2320	5741	3753	32	1.0	144	158	552	67	1.45	0.0122
-36%	2320	5741	3753	32	1.0	144	158	552	67	1.60	0.0110
-30%	2320	5741	3753	32	1.0	144	158	552	67	1.75	0.0101
-24%	2320	5741	3753	32	1.0	144	158	552	67	1.90	0.0093
-18%	2320	5741	3753	32	1.0	144	158	552	67	2.05	0.0086
-12%	2320	5741	3753	32	1.0	144	158	552	67	2.20	0.0080
-6%	2320	5741	3753	32	1.0	144	158	552	67	2.35	0.0075
0%	2320	5741	3753	32	1.0	144	158	552	67	2.50	0.0071

Variant	Capacity Ratios - NLYL Method				Capacity Ratios - Independent Design Checks (IDC)			
	D/C <sub>OYL</sub>	D/C <sub>OYL</sub> (Stiff Gst)	D/C <sub>UYL</sub>	D/C <sub>UYL</sub> (Stiff Gst)	D/C <sub>Rstr Bkl</sub>	D/C <sub>Guss Bkl</sub>	D/C <sub>Conn</sub>	Max D/C <sub>IDC</sub>
Base	0.97	0.36	0.09	0.07	1.00	0.70	0.99	1.00
-60%	1.52	0.56	0.12	0.10	1.00	0.70	0.99	1.00
-54%	1.40	0.52	0.11	0.09	1.00	0.70	0.99	1.00
-48%	1.31	0.48	0.11	0.09	1.00	0.70	0.99	1.00
-42%	1.24	0.46	0.10	0.09	1.00	0.70	0.99	1.00
-36%	1.18	0.44	0.10	0.08	1.00	0.70	0.99	1.00
-30%	1.13	0.42	0.10	0.08	1.00	0.70	0.99	1.00
-24%	1.09	0.40	0.09	0.08	1.00	0.70	0.99	1.00
-18%	1.05	0.39	0.09	0.08	1.00	0.70	0.99	1.00
-12%	1.02	0.38	0.09	0.08	1.00	0.70	0.99	1.00
-6%	1.00	0.37	0.09	0.07	1.00	0.70	0.99	1.00
0%	0.97	0.36	0.09	0.07	1.00	0.70	0.99	1.00
Max	1.52	0.56	0.12	0.10	1.00	0.70	0.99	1.00

### 3.11 Varying the Initial Imperfection Angle of the Insertion Zone (θ<sub>0</sub>)

The initial imperfection angle of the insertion zone results primarily from the debonding gap provided by the manufacturer, considered over the embedment length. This angle contributes directly to the total imperfection angle which determines the notional load that creates demand on the system as discussed in the

previous section. This angle is calculated as the total manufacturer's debonding gap divided by the neck insertion length and, as such, varying this angle is identical to varying the debonding gap (i.e. doubling the gap will double the angle, etc). Results of varying this angle are shown in Figure 14 and Table 11. Here also, the considered range of variations was taken somewhat larger than typical so that trends can be expressed. It can be seen from Figure 11 that for values of initial imperfection just slightly larger than the base manufacturer tolerance both the NLYL method (OYL mode) and the IDC method's OOP casing check (as adapted from Xie) produce results that exceed unity. This is again a sign of the efficiency of the base design and the balance that must be achieved in BRB design (as discussed in the previous section). However, it should not be expected for the manufacturer's gap to exceed much past the base value (ideal manufacturers gap) as this would violate tested parameters and likely result in other undesirable behaviour. But the results emphasise the importance of achieving, and maintaining, the proper debonding gap with values of the gap of only around 10% over that of the base value leading to unacceptable results in this particular case.

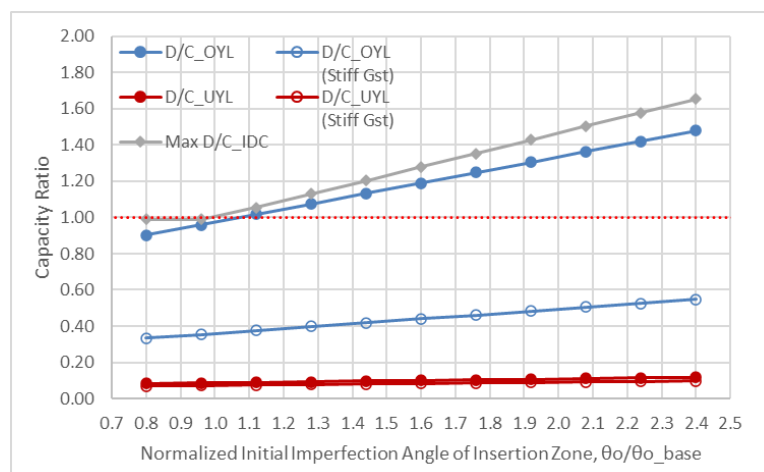


Figure 14: Effects of varying the initial imperfection angle of the insertion zone ( $\theta_0$ ).

Table 11: Effects of varying the initial imperfection angle of the insertion zone ( $\theta_0$ ).

Parameters Considered											
Variant	N*	L <sub>0</sub>	N <sup>B</sup> <sub>cr</sub>	t <sub>g</sub>	K <sub>b</sub>	W <sub>t</sub>	W <sub>1</sub>	ξL <sub>0</sub>	L <sub>AVE</sub>	Embed Ratio	θ <sub>0</sub>
	kN	mm	kN	mm		mm	mm	mm	mm		rad
Base	2320	5741	3753	32	1.0	144	158	552	67	2.50	0.0071
-20%	2320	5741	3753	32	1.0	144	158	552	67	2.50	0.0057
-4%	2320	5741	3753	32	1.0	144	158	552	67	2.50	0.0068
+12%	2320	5741	3753	32	1.0	144	158	552	67	2.50	0.0079
+28%	2320	5741	3753	32	1.0	144	158	552	67	2.50	0.0090
+44%	2320	5741	3753	32	1.0	144	158	552	67	2.50	0.0102
+60%	2320	5741	3753	32	1.0	144	158	552	67	2.50	0.0113
+76%	2320	5741	3753	32	1.0	144	158	552	67	2.50	0.0124
+92%	2320	5741	3753	32	1.0	144	158	552	67	2.50	0.0136
+108%	2320	5741	3753	32	1.0	144	158	552	67	2.50	0.0147
+124%	2320	5741	3753	32	1.0	144	158	552	67	2.50	0.0158
+140%	2320	5741	3753	32	1.0	144	158	552	67	2.50	0.0170

Variant	Capacity Ratios - NLYL Method				Capacity Ratios - Independent Design Checks (IDC)			
	D/C <sub>OYL</sub>	D/C <sub>OYL</sub> (Stiff Gst)	D/C <sub>UYL</sub>	D/C <sub>UYL</sub> (Stiff Gst)	D/C <sub>Rstr Bkl</sub>	D/C <sub>Guss Bkl</sub>	D/C <sub>Conn</sub>	Max D/C <sub>IDC</sub>
Base	0.97	0.36	0.09	0.07	1.00	0.70	0.99	1.00
-20%	0.90	0.33	0.08	0.07	0.91	0.70	0.99	0.99
-4%	0.96	0.35	0.09	0.07	0.98	0.70	0.99	0.99
+12%	1.02	0.38	0.09	0.08	1.05	0.70	0.99	1.05
+28%	1.08	0.40	0.09	0.08	1.13	0.70	0.99	1.13
+44%	1.13	0.42	0.10	0.08	1.20	0.70	0.99	1.20
+60%	1.19	0.44	0.10	0.08	1.28	0.70	0.99	1.28
+76%	1.25	0.46	0.10	0.09	1.35	0.70	0.99	1.35
+92%	1.31	0.48	0.11	0.09	1.43	0.70	0.99	1.43
+108%	1.36	0.50	0.11	0.09	1.50	0.70	0.99	1.50
+124%	1.42	0.53	0.11	0.10	1.58	0.70	0.99	1.58
+140%	1.48	0.55	0.12	0.10	1.65	0.70	0.99	1.65
Max	<b>1.48</b>	<b>0.55</b>	<b>0.12</b>	<b>0.10</b>	<b>1.65</b>	<b>0.70</b>	<b>0.99</b>	<b>1.65</b>

## 4 SUMMARY

The NLYL method for global BRB stability was compared to independent design checks performed on BRBs. Eleven parameters were varied in isolation to evaluate the sensitivity of each for the different design methods. The methods generally gave similar and supporting results. Compact gussets were analysed with a 2.5% OOP story drift and for cases with and without gusset stiffeners attached. Stiffened gussets result in considerably improved results, though these benefits decrease for extended gussets with tapered profiles. Extended gussets with tapered profiles, and particularly those without additional stiffening, present a special concern that should be investigated with advanced methods. The assumed brace out-of-straightness factor of  $L/500$  appeared to be conservative, and the effects of casing stiffness seemed to not be accounted for adequately, producing additional conservatism. The manufacturer's debonding gap must be controlled carefully and provided in such a manner that it will be maintained over time and through repeated cycles.

## 5 REFERENCES

- AISC 2022 *Seismic Provisions for Structural Steel Buildings*, ANSI/AISC 341-22, American Institute of Steel Construction, Chicago, IL (pending release)
- Bruneau, M. Uang, C.M. & Sabelli, R (2<sup>nd</sup> Edition) 2011, *Ductile Design of Steel Structures*, New York City: McGraw-Hill Education
- Dowswell, B. 2006, *Effective length factors for gusset plate buckling*, AISC Engineering Journal, Second Quarter, 91-101.
- Dowswell, B. 2012, *Effective length factors for gusset plates in chevron braced frames*, Technical Note, AISC Engineering Journal, Third Quarter, 115-117.
- Dowswell, B. 2016, *Advances in Steel Construction Analysis*, 2016 NASCC (the Steel Conference) Proceedings.
- Matsui, R. Takeuchi, T. Nishimoto, K. Takahashi, S. & Ohyama, T. 2010, *Effective buckling length of buckling restrained braces considering rotational stiffness at restrainer ends*, 7<sup>th</sup> International Conference on Urban Earthquake Engineering & 5<sup>th</sup> International Conference on Earthquake Engineering, Proceedings 1049-1058
- Saxey, B. Vidmar, Z. Li, C.-H. Reynolds, M. & Uang, C.-M., 2019, *Predicting low-cycle fatigue life of buckling-restrained braces*, Pacific Conference on Earthquake Engineering, Proceedings.
- Saxey, B. Vidmar, Z. Li, C.-H. Reynolds, M. & Uang, C.-M., 2020, *A predictive low-cycle fatigue model of buckling-restrained braces*, 17<sup>th</sup> World Conference on Earthquake Engineering, Proceedings (in Review).
- Takeuchi, T. Matsui, R. Tada, T. & Nishimoto, K. 2012, *Out-of-plane stability of buckling-restrained braces including their connections*, 15<sup>th</sup> World Conference on Earthquake Engineering, Proceedings
- Takeuchi, T. Ozaki, H. Matsui, R. & Sutcu, F. 2014, *Out-of-plane stability of buckling-restrained braces including moment transfer capacity*, Earthquake Engineering & Structural Dynamics, 43(6), 851-869
- Takeuchi, T. & Wada, A 2017, *Buckling-restrained braces and applications*, Tokyo: The Japan Society of Seismic Isolation (JSSI)
- Thornton, W.A. 1984, *Bracing connections for heavy construction*, AISC Engineering Journal, Third Quarter, 139-148.
- Thornton, W.A. & Lini, C. 2011, *The whitmore section*, Modern Steel Construction, July 2011
- Xie, Quang 2005, State of the art of buckling-restrained braces in Asia. *Journal of Constructional Steel Research*, 61, 727-748
- Zaboli, B. Clifton, G.C. & Cowie K. 2018, BRBF and CBF gusset plates: Out-of-plane stability design using a simplified notional load yield line (NLYL) method. *Journal of the Structural Engineering Society of NZ*, 31(1), 64-76